

# DUAL SCALE FLOW DURING VACUUM INFILTRATION OF FIBER-REINFORCED COMPOSITES: FROM IN SITU SYNCHROTRON EXPERIMENTS TO NUMERICAL SIMULATIONS

Joaquí Vilà<sup>1</sup>, Federico Sket<sup>2</sup>, Carlos González<sup>3</sup>, Javier LLorca<sup>4</sup>

<sup>1</sup>IMDEA Materials Institute, 28906 - Getafe, Madrid, Spain

Email: joquim.vila@imdea.org, Web Page: <http://www.imdea.materials.org>

<sup>2</sup>IMDEA Materials Institute, 28906 - Getafe, Madrid, Spain. Email: federico.sket@imdea.org

<sup>3</sup>IMDEA Materials Institute, 28906 - Getafe, Madrid, Spain & Polytechnic University of Madrid, 28040 - Madrid, Spain. Email: carlosdaniel.gonzalez@imdea.org

<sup>4</sup>IMDEA Materials Institute, 28906 - Getafe, Madrid, Spain & Polytechnic University of Madrid, 28040 - Madrid, Spain. Email: javier.llorca@imdea.org

**Keywords:** Vacuum-assisted resin infusion, X-ray microtomography, dual flow

## Abstract

This presentation is a contribution to understand the phenomena that control vacuum-assisted resin infusion at the mesoscopic and microscopic scales. The mesoscopic behavior was studied by means of standard vacuum-assisted resin infusion tests. Fluid pressure was measured by means of pressure gages at different locations and the evolution of the out-of-plane displacement of the vacuum bag (due to changes in the fabric compaction) was continuously measured by means of the digital image correlation. In addition, infusion at the microscale was analyzed by means of in situ infiltration experiments carried out in the synchrotron beam. The high resolution of the X-ray tomography images allowed the detailed reconstruction of individual fibers within the tow while the contrast between the different phases (air, fluid and fibers) was enough to track the fluid front position and shape as well as the void transport during infiltration. This information was used to develop a level set based model to simulate fluid flow and fabric compaction during vacuum-assisted infusion. Fluid infusion through the fiber preform was modeled using Darcy's equations for the fluid flow through a porous media. The stress partition between the fluid and the fiber bed was included by means of Terzaghi's effective stress theory. These equations are only valid in the infused region and both regions (dry and wet) were separated by introducing a level set function in the partial differential equation which is defined at any given time as the distance to the flow front. Finally, the model predictions were validated against the experimental results.

## 1. Introduction

Vacuum-Assisted Resin Infusion (VARI) is an open mold liquid processing technique for composite materials. The upper part of the mold is replaced by a flexible bag and the resin is infiltrated into the fabric preform under the action of the atmospheric pressure. Fluid flow during VARI is mainly controlled by the competition between fabric compaction and fluid permeability. Before impregnation, the atmospheric pressure over the vacuum bag is directly transferred to the dry fiber network leading to compaction of the laminate. As the fluid infiltrates the fiber preform, the atmospheric pressure is shared between the fiber network and the fluid resulting in the well-known elastic spring back effect. The stress transfer mechanisms between the fluid and the fiber network strongly influence the mesoscopic flow because the preform compaction and the permeability are no longer homogeneous in the infused part,

leading to important changes in the pressure distribution, fluid velocity and filling times [1].

While large components can be manufactured by VARI (such as such as wind turbine blades, naval hulls and decks, bridge decks, etc.), optimization of infiltration during VARI from the viewpoint of thickness control and porosity is a challenging task. In particular, macrodefects results from dry or poorly impregnated regions that appear when the resin flow reaches the outlet gate prior to complete the filling stage due to an incorrect spatial distribution of the injection/infusion/venting ports [2, 3]. Even if the part has been completely filled with resin, voids can be generated in the material due to the inhomogeneous fluid flow caused by the dual scale of the porosity in the textile preform. Standard reinforcements used in composite manufacturing are produced by weaving tows containing thousands of fibers forming specific fabric architectures (woven, non-crimp, stitched, etc.). The initial free spaces in between individual fibers and between adjacent tows are considered, respectively, micro and mesoscale porosity.

Therefore, the global flow can be divided into mesoflow and microflow (Fig.1) Mesoflow takes place through the high permeability channels between adjacent fiber tows and it is mainly driven by the external pressure gradients and the fabric permeability. Microflow takes place within fiber tows and is mainly controlled by capillary forces. This dual-scale flow (micro-meso) is responsible of the generation of voids in composite materials by the direct competition between viscous and capillary forces [4, 5]. Experimental results demonstrated that void formation in engineering composites depends on the ratio between viscous and capillary forces through the non-dimensional modified capillary number,  $Ca^*$  [6, 7]

$$Ca^* = \frac{\mu v}{\gamma \cos \theta}. \quad (1)$$

where  $\mu$  and  $v$  stand for the resin viscosity and the average resin velocity, respectively, while  $\gamma$  and  $\theta$  are the fluid surface tension and the contact angle, respectively. Capillary numbers for an optimum void content in specific material systems have been reported [7]. Viscous forces are predominant over capillary ones for high capillary numbers ( $Ca^* > 10^{-2}$ ), and the rapid flow propagation along the yarn-to-yarn free gaps leads to the development of void entrapments at the intra-tow level (Fig. 1c). On the contrary, the fluid velocity is small for low capillary numbers ( $Ca^* < 10^{-3}$ ) and the wicking effects caused by the intratow capillary forces become predominant. In this latter case, entrapments are generated at the tow interfaces rather than at the intratow spaces (Fig. 1a). The appropriate range of filling rate (given by the capillary number) with uniform progress of both flows would lead to a minimization of the void formation in the material (Fig. 1b). Mesovoids can be easily reduced by selecting the appropriate venting strategy and controlling the pressure gradients within the fabric preform. However, microvoids are more difficult to evacuate due to the surface tension forces acting at the fiber bundle scale. As a result, microvoids will tend to be confined in areas with low pressure gradients. Understanding the mechanisms of resin flow at meso and microlevel during liquid molding is crucial to manufacture high quality composite parts with low fraction of voids and defects and this was the main objective of this investigation.

## 2. Microflow characterization by synchrotron X-ray tomography

Infusion at the microscale was analyzed by means of *in situ* infiltration experiments carried out in the synchrotron beam [8]. The high resolution of the X-ray tomography images allowed the detailed reconstruction of individual fibers within the tow while the contrast between the different phases (air, fluid and fibers) was enough to track the fluid front position and shape as well as the void transport during infiltration (Fig. 2). The high resolution images provided by X-ray microtomography showed an obtuse contact angle between the fluid and the fibers at the flow front. This behavior, which was opposed to the wetting

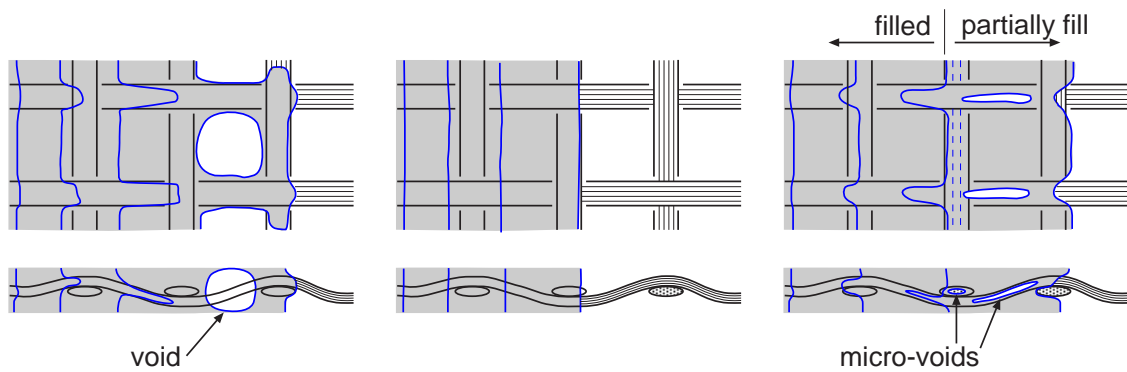


**Figure 1.** Schematic of the development of porosity due to dual flow during liquid resin infusion of fiber preforms. (a)  $Ca^* < 10^{-3}$ . (b)  $10^{-3} < Ca^* < 10^{-2}$ . (c)  $Ca^* > 10^{-2}$ .

contact angles measured in air, was also reported by other authors [9, 10] and it cannot be attributed to dynamic effects because the tomograms were acquired when the flow front was stopped. More likely, it seems to be a surface effect triggered in vacuum by the interaction between the fluid and the fiber sizing. One consequence of the phenomenon is that the capillary pressure acted as a drag force on the fluid flow. As a result, fluid flow was favored through areas with low fiber volume fraction which presented higher permeability and lower capillary forces. The complexity of the microflow depended markedly on the microstructure and the presence of convergent/divergent individual fiber trajectories played a significant role. Convergent fiber trajectories tend to arrest the fluid propagation by capillary forces and the detailed reconstruction of the fiber distribution allowed the interpretation of the flow progression in terms of the capillary pressure and permeability factors.

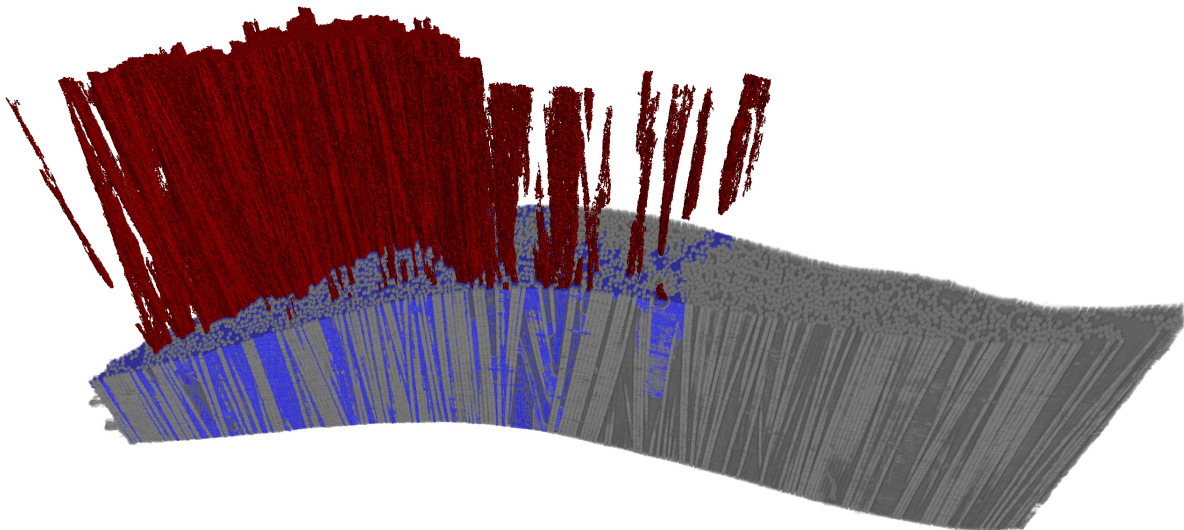


**Figure 2.** 3D tomogram of the fiber tow during infiltration. Matrix and glass fibers are shown in dark and light grey, respectively. The macroscopic pore, which is crossing through the tow, is shown in red while the fluid is presented in navy blue.

The transport of small and large voids was also assessed by means of X-ray microtomography. Small

voids were transported along the tow direction through the empty spaces between individual fibers. They were trapped when the distance between fibers was below a critical value because the pressure gradient required to overcome the capillary pressure was too high. As a result, a large volume fraction of very small voids was trapped in the microstructure. The propagation of a large void spanning dozens of fibers was also observed in the experiments. In this case, the void migrated easily along the fiber tow driven by the vacuum pressure gradient. Very interestingly, the internal pressure of the void was large enough to produce significant fiber and bag movements during the void transport, leaving a trail of smaller voids in the wake [11].

### 3. Mesoflow characterization and modeling

Mesoflow was studied by means of standard VARI tests. The experimental set-up for the infusion tests is sketched in Figure 3, leading to an approximate unidimensional flow between the inlet and outlet gates. Fiber preforms with three different thicknesses ( $[0]_2$ ,  $[0]_4$ ,  $[0]_8$  stacking sequences) were infiltrated. The displacement field (or the variation of the fabric thickness  $h(x,t)$  during the infusion experiments) was measured by means of digital image correlation. To this end, a speckle pattern was painted on the vacuum bag surface using a white painting with a fine dispersion of black dots. The speckle pattern was deposited after several vacuum/release cycles in order to mitigate as much as possible nesting effects between fabric layers during the infusion experiments. The area of interest, AOI, (region where digital image correlation is performed) was restricted to a central strip of  $210 \times 10 \text{ mm}^2$  aligned with the flow direction. Unidimensional fluid flow was reported in most of the tests: uniform along the width of the strip without significant race-tracking along the fabric edges. More details can be found in [11, 12].

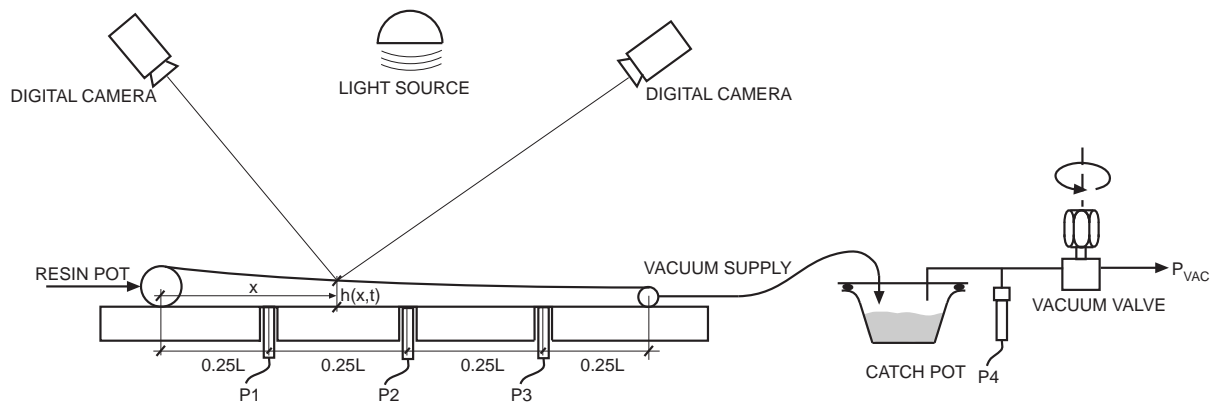


**Figure 3.** Sketch of the experimental infusion set-up and of the digital image correlation system.

The experimental results provided a very detailed picture of the interaction between fluid infiltration mechanisms and preform deformation during unidirectional, in-plane flow. In general, filling times and flow progression mechanisms were independent of the fabric thickness. A slight reduction of the fabric thickness was detected at the flow front due to the lubrication of the fiber bed. Afterwards, the bag thickness increased continuously at each point of the infusion length until a maximum value as the stress was progressively transfer from the fiber bed to the infusion fluid and the fabric permeability increased accordingly. The bag displacement increased as the distance to the inlet gate decreased and the shape of the vacuum bag during infusion was controlled by the complex interaction between permeability and compaction during infiltration controlled the evolution of the non-linear shape of the vacuum bag during the infusion (Fig. 4a). The pressure in the fluid increased rapidly towards an asymptotic value once the

steady state regime was established and the whole fabric was filled by the fluid (Fig. 4b).

The mesoscale fluid flow and fabric compaction during VARI of composite materials was simulated by means of a level set model. Fluid infusion through the fiber preform was modeled using Darcy's equations for the fluid flow through a porous media, including the continuity condition. The stress partition between the fluid and the fiber bed was included by means of Terzaghi's effective stress theory, leading to a non-linear partial differential equation. This equation is only valid in the infused region and it was necessary to separate both regions. This was achieved by introducing a level set function  $\phi$  in the partial differential equation which is defined at any given time as the distance to the flow front. Obviously, the flow front is identified by the condition  $\phi = 0$  and tracking the fluid front is equivalent to finding the zero level of the evolving function during infusion by solving a hyperbolic partial differential equation. The partial differential equations were discretized and solved approximately using the finite differences method with a uniform grid discretization of the spatial domain. Darcy's equation was solved using a standard Euler method for the time integration and a central differences algorithm for the spatial integration. The time integration of the level set equation was approximated with the forward Euler method while the upwind algorithm was used for the spatial integration to account for the hyperbolic nature of the evolution equation [12].

The model predictions were validated against the results of the VARI tests in the  $[0]_8$  E-glass plain woven preform. The evolution of the flow front and of the fabric thickness during infusion were measured by means of digital image correlation while the fluid pressure at various locations was monitored with pressure gages. The physical parameters of the model, including the fluid viscosity  $\mu$ , in-plane fabric permeability  $\mathbf{K} = \mathbf{K}(V_f)$  and fiber bed compressibility, were also independently measured. The model results (in terms of fabric thickness, pressure and fluid front evolution) were in good agreement with the experimental data, Figure 4, showing the potential of the level set method to simulate resin infusion.

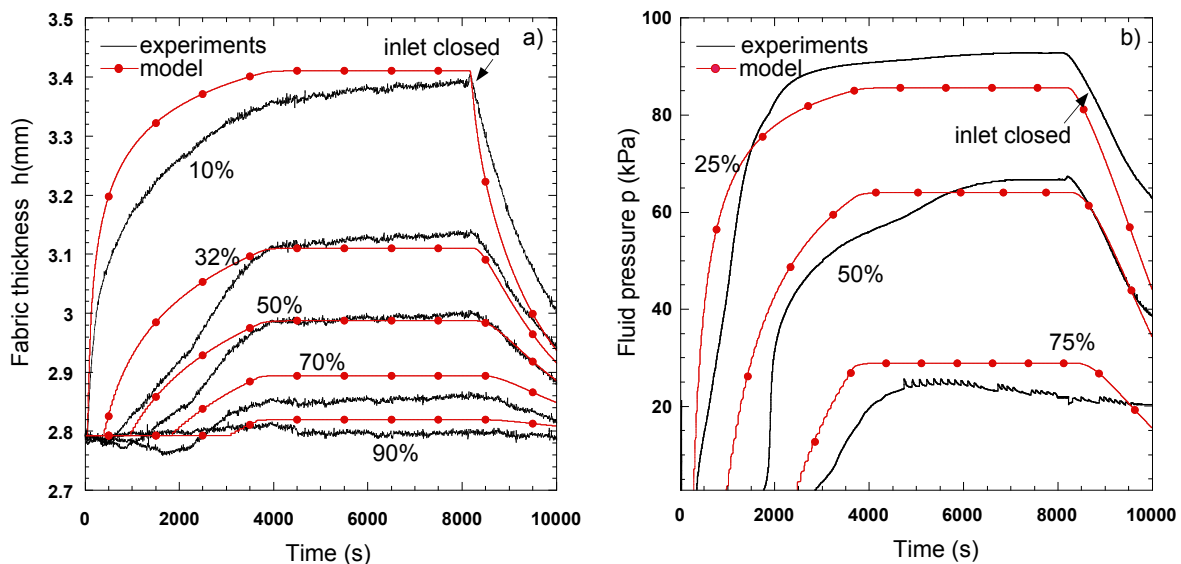


**Figure 4.** Experimental and simulation results of the VARI experiments in an  $[0]_8$  E-glass plain woven preform. (a) Variation of the fabric thickness,  $h$ , as a function of the filling time at different locations along the infusion length (10, 32, 50, 70 and 90% of the strip of 210 mm in length). (b) Evolution of the fluid pressure at at different locations along the infusion length (25, 50 and 75% of the strip of 210 mm in length).

## Acknowledgments

This investigation was supported by the Ministerio de Economía y Competitividad of Spain through the grant MAT2012-37552.

## References

- [1] B. Yenilmez, M. Senan, and E. Murat Sozer. Variation of part thickness and compaction pressure in vacuum infusion process. *Composites Science and Technology*, 69:1710–1719, 2009.
- [2] E. Ruiz, V. Achim, S. Soukane, F. Trochu, and J. Bréard. Optimization of injection flow rate to minimize micro/macro-voids formation in resin transfer molded composites. *Composites Science and Technology*, 66:475–486, 2006.
- [3] J. S. U. Schell, M. Deleglise, C. Binetruy, P. Krawczak, and P. Ermanni. Numerical prediction and experimental characterisation of meso-scale-voids in liquid composite moulding. *Composites Part A: Applied Science and Manufacturing*, 38:2460–2470, 2007.
- [4] J. M. Lawrence, V. Neacsu, and S. G. Advani. Modeling the impact of capillary pressure and air entrapment on fiber tow saturation during resin infusion in LCM. *Composites Part A: Applied Science and Manufacturing*, 40:1053–1064, 2009.
- [5] N. Patel and L. J. Lee. Modeling of void formation and removal in liquid composite molding. Part I: Wettability analysis. *Polymer Composites*, 17:96–103, 1996.
- [6] C. Ravey, E. Ruiz, and F. Trochu. Determination of the optimal impregnation velocity in Resin Transfer Molding by capillary rise experiments and infrared thermography. *Composites Science and Technology*, 99:96 – 102, 2014.
- [7] Y. K. Hamidi, L. Aktas, and M. C. Altan. Formation of microscopic voids in resin transfer molded composites. *Journal of Engineering Materials and Technology*, 126:420–426, 2004.
- [8] J. Vilà, F. Sket, F. Wilde, G. Requena, C. González, and J. LLorca. An *in situ* investigation of microscopic infusion and void transport during vacuum-assisted infiltration by means of x-ray computed tomography. *Composites Science and Technology*, 119:12–19, 2015.
- [9] M. Li, S. Wang, Y. Gu, Z. Zhang, Y. Li, and K. Potter. Dynamic capillary impact on longitudinal micro-flow in vacuum assisted impregnation and the unsaturated permeability of inner fiber tows. *Composites Science and Technology*, 70:1628–1636, 2010.
- [10] J. Verrey, V. Michaud, and J.A.E. Manson. Dynamic capillary effects in liquid composite moulding with non-crimp fabrics. *Composites: Part A*, 37:92–102, 2006.
- [11] J. Vilà. *Dual scale flow during vacuum infusion of composites: experiments and modelling*. PhD thesis, Carlos III University of Madrid, 2016.
- [12] J. Vilà, C. González, and J. LLorca. A level set approach for the analysis of flow and compaction during resin infusion in composite materials. *Composites Part A: Applied Science and Manufacturing*, 67:299–307, 2014.